First test on Photonic Crystal Fiber potential for broadband interferometry

Sébastien Vergnole, Laurent Delage, François Reynaud, Laurent Labonté, Philippe Roy, G. Melin, L. Gasca

First test on Photonic Crystal Fiber potential for broadband interferometry

Sébastien Vergnole, Laurent Delage, and François Reynaud

IRCOM OCNL (UMR CNRS 6615), 123 ave. A. Thomas, 87 060 LIMOGES Cedex, FRANCE

Laurent Labonté, and Philippe Roy

IRCOM OGI (UMR CNRS 6615), 123 ave. A. Thomas, 87 060 LIMOGES Cedex, FRANCE

Gilles Mélin, and Laurent Gasca

ALCATEL Research and Innovation, 91 461 MARCOUSSIS, FRANCE

The Photonic Crystal Fibers (PCFs) are microstructured waveguides currently developed in the frame of metrology, non-linear optics or coherent tomography. PCF studies are mainly focused on the improvement of dispersion property and wide spectral single-mode operating domain. Consequently, in the astronomical context, this kind of fiber is a good candidate to design a fiber linked version of stellar interferometer for aperture synthesis. In this paper, we study the potential of these fibers taking advantage of the wide spectral single-mode operation. We propose an experimental setup acting as a two-beam interferometer using PCFs to measure fringes contrasts at four different wavelengths (670nm, 980nm, 1328nm and 1543nm) corresponding to R, I, J and H astronomical bands with the same couple of PCFs. For this purpose, we implement for the first time a piezoelectric PCF optical path modulator.

OCIS codes: 060.2430, 120.3180, 350.1270

1. Introduction

Photonic Crystal Fibers (PCFs) have been intensively studied during these last few years. Actually, the main application of PCFs are metrology,[1] non-linear optics[2] or coherent tomography.[3] These fibers consist of a pure silica core surrounded by a silica-air photonic crystal acting as a cladding. This cladding typically consists of thin cylindrical air holes running along the fiber axis in a silica bulk material. The guiding process results from a refractive index difference between core and cladding due to air holes of the photonic crystal. Since the experimental feasibility of PCFs has been demonstrated,[4] it is possible to experimentally investigate their use in the frame of interferometry and aperture synthesis in astronomy. The single-mode propagation property over a very large spectral range[5,6] allows a significant simplification for the implementation of a fiber linked interferometer. For example, it is possible to design a single-mode waveguide operating over 1 μm spectral bandwidth from 0.6 μm to 1.6μm. With such characteristics, only one fiber would be required for each fiber arm when a set of three or four classical fibers would be necessary for the same feature as, for example, for 'OHANA project[7] (Fig. 1).
The scope of this paper is to validate the ability of PCFs to propagate very large spectrum in a single-mode operation and to test their capabilities to operate in a broadband interferometric context. For this purpose, a PCF optical path modulator has been implemented for the first time to our knowledge.

2. Experimental setup

The experimental setup is shown figure 2. A set of four broadband sources allows us to scan a large spectral domain corresponding to the R, I, J and H astronomical bands. The setup is fed by one of the four sources (Fabry-Perot laser diode under or beyond the lasing threshold) located at the input of a broadband beamsplitter. Laser diode mean wavelength and Full Width at Half Maximum (FWHM) are listed in table 1. The emerging beams reach the launching assemblies constituted of off-axis parabolas. Their achromatic properties enable an efficient coupling in the PCFs over the whole spectral domain. Nevertheless, the numerical aperture is wavelength dependent. In our experiment the injection process is optimized around 670nm and a detailed analysis all over the operating spectrum is planned for future applications. The two fiber arms are constituted of two 10-meter-long PCFs manufactured by ALCATEL. These fibers consist of a pure silica core surrounded by a photonic crystal acting as a cladding. This cladding is made with a triangular lattice of four layers of thin cylindrical air holes running along the fiber axis in a silica bulk material. Their main characteristics are the air hole diameter: $d = 1.9\mu m \pm 0.1\mu m$, and the pitch which is the distance between air hole center: $\Lambda = 2.3\mu m \pm 0.1\mu m$. Figure 3 shows the transverse section of PCFs used.

The chromatic dispersion has been measured thanks to low coherence interferometric principle.[8] It has been also determined by calculations based on Finite Element Method. Experimental and theoretical curves are plotted figure 4.

It must be kept in mind that this PCF is not specially designed for stellar interferometry, thus, characteristics are not optimized for this application. Anyway, the interferometer quality and the fringe contrasts are not linked with the intrinsic properties of fibers but with the homogeneity between both fiber arms of the interferometer. These are not the intrinsic parameters which are important but parameters fluctuations between both arms. Thus, our experiment aims at characterizing their homogeneity rather than their intrinsic properties.

As far as the attenuation is concerned, it remains steady over the operating domain (except for the OH peak around 1400nm) and no bending losses have been observed whatever the wavelength with bending radius greater than 4mm. This is due to the large air/silice ratio of these PCFs. Even if the level of attenuation of our fiber is rather high, around $40dB/km$, polarization maintaining PCFs are now available commercially with attenuation in the same range as conventional fibers (around few dB/km[9]).

Taking advantage of our experience on conventional fiber,[10] we implemented on one of the two arms an optical fiber modulator with a $70\mu m$ stroke calibrated with an almost monochromatic source ($\Delta\lambda = 2.5nm$)(Fig. 5). This device uses a stretching process: PCF is wound onto a 6cm diameter cylindrical piezoelectric actuator. As these PCFs have no bending losses, the transmission remains steady during the stretching. This stretching is weakly non-linear and it is possible to servo-control the optical path modulation to be linear as for conventional fibers.[10] It is the first time to our best knowledge that such a device has been implemented.

An air delay line allows the instrument to operate around the zero group delay. A 1.3cm air path difference has been measured between the two arms.

The emerging beams coming from the PCF waveguides are mixed by means of a broadband beamsplitter. The output of the Mach-Zehnder interferometer is sent to detectors dedicated to the different spectral channels.

Although these PCFs are not designed to be polarization maintaining, they exhibit highly birefringence properties due to the manufacturing process which induced slight geometrical default and stress along the fiber. Labonté et al.[11] have made experimental and theoretical analysis of the birefringence in such fibers. A birefringence of $\Delta n = 1.2 \cdot 10^{-3}$ at $\lambda = 1550nm$ has been measured. Therefore, these PCFs are highly birefringent and both principal axes of polarization of the fibers have to be aligned at the input and the output of the interferometer.

A polarizer selects a linear polarization parallel to a fiber principal axis of polarization so that the instrument operates along one polarization mode. The polarization preserving properties have been preliminary tested. We have experimentally observed a 20.0dB extinction ratio for one fiber arm and a 13.6dB for the other one. These ratio will involve a weak contrast loss. The difference in extinction ratio between both arms comes from the experimental inhomogeneity of the fibers.

3. Experimental results

The evaluation of the ability of PCF to operate in the interferometric context over a broadband spectrum has been evaluated by fringes contrast measurements which is defined by:

$$Contrast = \frac{I_{max} - I_{min}}{I_{max} + I_{min}}. \tag{1}$$

where I_{max} stands for the maximum intensity of the fringe pattern and I_{min} is the minimum intensity.

The optimization of the visibility function necessitates to control different parameters. The polarization coherence is mainly preserved thanks to the alignment of the principal axes of the fibers and launching a linearly polarized source along one principal axis. The differential dispersion effects have been minimized by cutting the fibers with a typical 5mm relative length accuracy. Nevertheless, the inhomogeneity of the waveguide and the imperfect equalization of the fiber length arms lead to a reduction of the fringe contrasts and to an observation of the interferograms at different positions of the delay line. Figures 6 and 7 show examples of normalized fringe pattern for extreme spectral bands.

Table 2 gives contrasts and delay positions for the different spectral bands.

Contrasts beyond the threshold are less than 100% due to the polarization effect. Under the threshold, we reached high fringes contrasts. Moreover, contrast difference between the two operating mode of the laser diode (broadband or laser emission) and delay line position show that differential chromatic dispersion is greater for 1328nm and 1543nm mean wavelengths than for 670nm and 980nm.

The experimental contrasts are comparable with those achieved with conventional fibers dedicated to one spectral band.[12–14]

Moreover, to point out the PCFs potential, we carried out experiment with a classical silica highly birefringent fiber with a 600nm cutoff wavelength. We fed this fiber with a 1328nm and 1543nm mean wavelength laser diode. We observed a tremendous attenuation and a very high sensitivity to bending. Consequently, it is impossible to use classical fibers on the same single-mode operating domain as PCFs.

4. Conclusion

These preliminary measurements have shown that PCFs are able to operate coherently in single-mode operation from 670nm to 1543nm (astronomical bands R, I, J and H). With

this kind of fibers, the implementation of a fiber linked broadband stellar interferometer is simplified: instead of using three or four set of fibers to cover a 1000nm spectral bandwidth, from 670nm to 1543nm, we will only use a single one.
Besides, we have implemented for the first time a PCF optical path modulator with a $70\mu m$ stroke and with no transmission losses. These properties made PCF very good candidate for application in aperture synthesis.
Of course, some remaining points need to be tested:

- the study of differential chromatic dispersion using our background on silica fibers,[13]
- to upgrade our interferometer in order to add a third arm and take phase closure measurements,[15,16]
- the implementation of a PCF delay line taking advantage of our experience on silica fiber delay line.[17] Besides, one of the potential of PCF is the low chromatic longitudinal dispersion which may allow to propose a low dispersive fiber delay line. This device would be an important feature for all-fibered astronomical delay line.
- design a special opto-geometrical configuration (hole diameter and pitch) to manufacture a PCF sample dedicated to stellar interferometry.[18]

At last, the following step will be to design an all-PCFs interferometer using PCF coupler under development.[19]

References

1. Holzwarth, R., Zimmermann, M., Udem, T., Hänsch, T. W., Russbüldt, P., Gäbel, K., Poprawe, R., Knight, J. C., Wadsworth, W. J., & Russell, P. S. J. , "White-light frequency comb generation with a diode-pumped Cr:LiSAF laser", Optics Letters 26, 1376-1378 (2001).
2. Champert, P. A., Couderc, V., & Barthélémy, A. , "Multi-watt, Continuous wave, continuum generation in dispersion shifted fiber by use of high power fiber source", presented at NonLinear Guided Waves and Their Applications, Toronto, Canada, 28-31 March 2004.
3. Wang, Y., Zhao, Y., Nelson, J. S., Chen, Z., & Windeler, R. S. , "Ultrahigh-resolution optical coherence tomography by broadband continuum generation from a photonic crystal fiber" , Optics Letters 28, 182-184 (2003).
4. Knight, J. C., Birks, T. A., Russell, P. S. J., & Atkin, D. M. , "All-silica single-mode optical fiber with photonic crystal cladding", Optics Letters 21, 1547-1549 (1996).
5. Birks, T. A., Knight, J. C., & Russell, P. S. J. , "Endlessly single-modephotonic crystal fiber", Optics Letters 22, 961-963 (1997).

6. Knight, J. C., Birks, T. A., Russell, P. S. J., & de Sandro, J. P. , "Properties of photonic crystal fiber and the effective index model", Journal of Optical Society of America A 15, 748-752 (1998).
7. Perrin, G., Lai, O., Lena, P. J., & Coude du Foresto, V. , "Fibered large interferometer on top of Mauna Kea: 'OHANA, the optical Hawaiian array for nanoradian astronomy", in *Interferometry in Optical Astronomy*, Pierre J. Lena and Andreas Quirrenbach, Eds., Proc. SPIE 4006, 708-714 (2000).
8. Diddams, S., & Diels, J. C. , "Dispersion measurements with white-light interferometry", Journal of Optical Society of America B 13, 1120-1129 (1996) .
9. These data are available at http://www.blazephotonics.com/
10. Reynaud, F. & Delaire, E. , "Linear optical path modulation with $\lambda/200$ accuracy using a fiber stretcher", Electronics Letters 29, 1718-1719 (1993).
11. Labonte, L., Bahloul, F., Roy, P., Pagnoux, D., Blondy, J. M., Auguste, J. L., Mélin, G., Gasca, L., & Zghal, M. , "Experimental and Numerical Analysis of the Birefringence into Microstructured Optical Fibres", in *Proceedings of European Conference on Optical Communication* (Stockholm, Sweden), pp. 70-71 (2004).
12. Reynaud, F. & Lagorceix, H. "Stabilization and control of a fiber array for the coherent transport of beams in a stellar interferometer", in *Proceedings of Integrated Optics for Astronomical Interferometry*, P. Kern and F. Malbet, eds. (Grenoble, France), pp. 249-253 (1996).
13. Vergnole, S., Delage, L., & Reynaud, F. , "Accurate measurements of differential chromatic dispersion and contrasts in an hectometric silica fibre interferometer in the frame of 'OHANA project", Optics Communications 232, 31-43 (2004).
14. Vergnole, S., Delage, L., & Reynaud, F. , "Measurements of differential chromatic dispersion and contrasts in an hectometric silica fibre interferometer in the frame of 'OHANA project", in *New Frontiers in Stellar Interferometry*, Proc. SPIE 5491 (2004), in press.
15. Rogstad, D. H. , "A Technique for Measuring Visibility Phase with an Optical Interferometer in the Presence of Atmospheric Seeing", Applied Optics 7, 585-588 (1968).
16. Delage, L., Reynaud F., & Lannes, A. , " Analysis and control of polarization effects on phase closure and image acquisition in a fibre-linked three-telescope stellar interferometer", Applied Optics 39, 6406-+ (2000).
17. Simohamed, L. M. & Reynaud, F. , "Characterisation of the dispersion evolution versus stretching in a large stroke optical fibre delay line", Optics Communications 159, 118-+ (1999).
18. Peyrilloux, A., Pagnoux, D., & Reynaud, F. , "Evaluation of photonic crystal fiber potential for fiber linked version of stellar interferometers", in *Interferometry for Optical Astronomy II.* Wesley A. Traub, ed., Proc. SPIE 4838, 1334-1340 (2003).

19. Lee, B. H., Eom, J. B., Kim, J., Moon, D. S., Paek, U., & Yang, G. , "Photonic crystal fiber coupler", Optics Letters 27, 812-814 (2002).

List of Figure Captions

Fig. 1 Stellar interferometer arms: (a) with conventional single-mode fiber, 4 kinds of fiber is needed for a 1000nm bandwidth, (b) with PCF, the same fiber is used from 600nm to 1600nm

Fig. 2 Experimental setup: PCFs Mach-Zehnder interferometer. P1, P2, P3: off-axis parabola. T1 and T2: 10-m long PCFs

Fig. 3 Transverse section of the PCFs used in our experiment

Fig. 4 Chromatic dispersion as a function of the wavelength: measurement and simulation. Simulation have been made taking into account the real shape of the hole. Thus, due to the image processing of the transverse section of the PCF, uncertainties exist ($\pm 5ps/(nm/km)$) but error bars for simulation are not plotted so as to keep the figure readable.

Fig. 5 Fringe pattern for 1543nm mean wavelength beyond the lasing threshold

Fig. 6 Fringe pattern for 670nm mean wavelength

Fig. 7 Fringe pattern for 1543nm mean wavelength

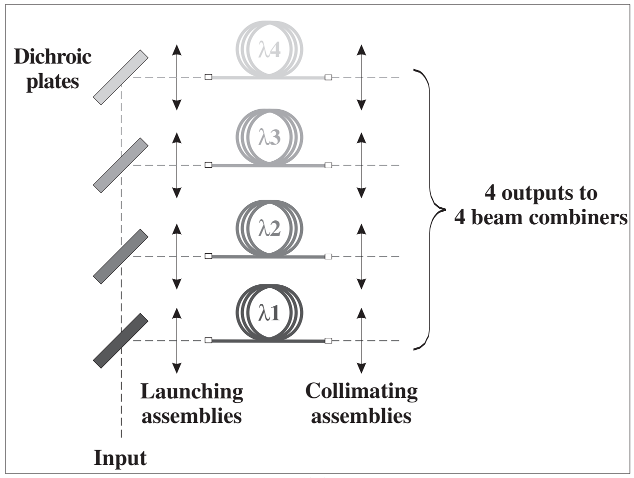
Dichroic plates
λ4
λ3
λ2
λ1
4 outputs to
4 beam combiners
Launching assemblies
Collimating assemblies
Input

(a)

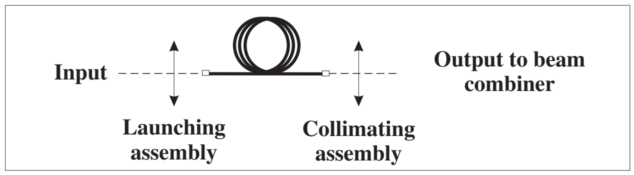
Input
Output to beam combiner
Launching assembly
Collimating assembly

(b)

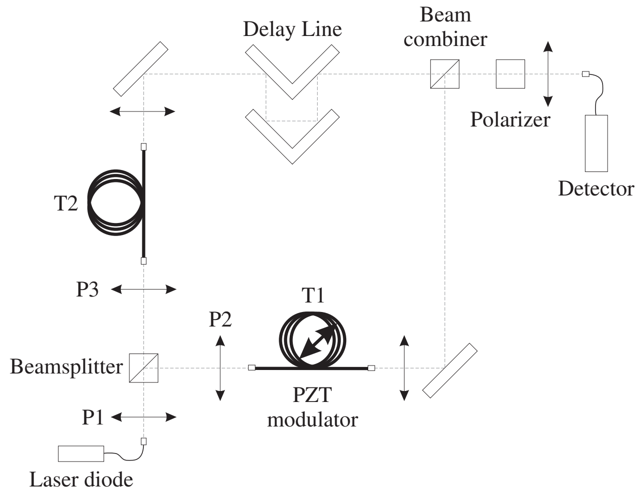
Delay Line
Beam
combiner
Polarizer
Detector
T2
P3
T1
P2
Beamsplitter
PZT
modulator
P1
Laser diode

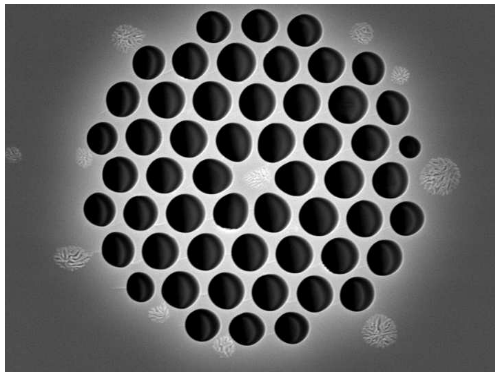

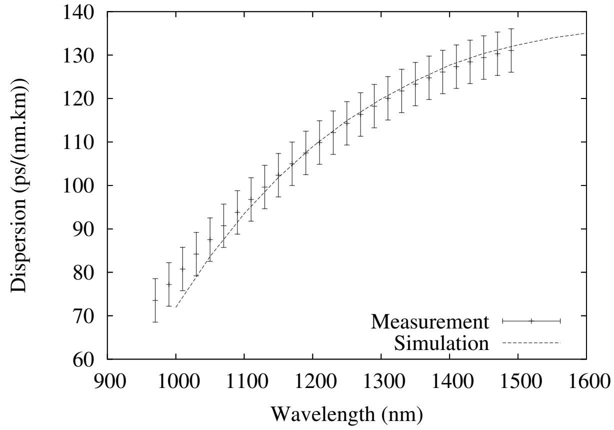
140
130
120
110
100
90
80
70
60
Dispersion (ps/(nm.km))
900
1000
1100
1200
1300
1400
1500
1600
Wavelength (nm)
Measurement
Simulation

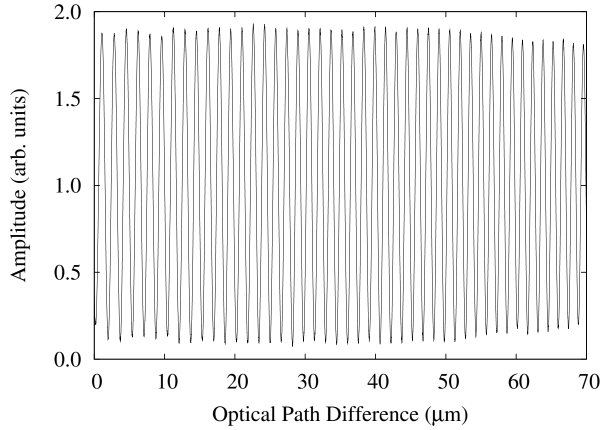
2.0
1.5
1.0
0.5
0.0
Amplitude (arb. units)
0
10
20
30
40
50
60
70
Optical Path Difference (µm)

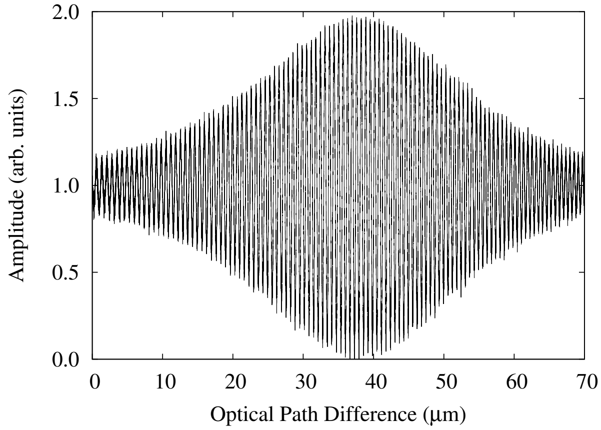
2.0
1.5
1.0
0.5
0.0
Amplitude (arb. units)
0
10
20
30
40
50
60
70
Optical Path Difference (μm)

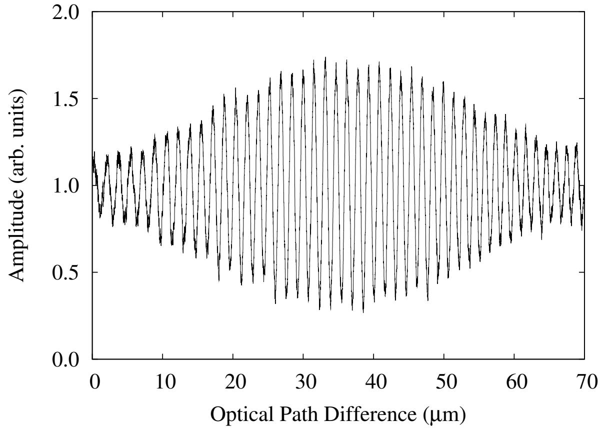
2.0
1.5
1.0
0.5
0.0
Amplitude (arb. units)
0
10
20
30
40
50
60
70
Optical Path Difference (μm)

Table 1. Sources used in our experiment

Mean Wavelength	FWHM under the threshold	Corresponding Astronomical Band
670 nm	8 nm	R $[0.59 - 0.81 \mu m]$
980 nm	10 nm	I $[0.78 - 1.02 \mu m]$
1328 nm	18 nm	J $[1.1 - 1.4 \mu m]$
1543 nm	26 nm	H $[1.4 - 1.8 \mu m]$

Table 2. Variation of contrast and delay line position as a function of the wavelength

Mean Wavelength	Measured Contrast		Delay Line Position
	beyond the threshold	under the threshold	(arbitrary origin)
670 nm	$95\% \pm 1\%$	$96\% \pm 1\%$	$0 \mu m$
980 nm	$88\% \pm 1\%$	$87\% \pm 1\%$	$20 \mu m$
1328 nm	$92\% \pm 1\%$	$83\% \pm 1\%$	$100 \mu m$
1543 nm	$93\% \pm 1\%$	$74\% \pm 1\%$	$200 \mu m$